

MODELING AND SIMULATION OF ARMORED WHEELED VEHICLES WITH FLEXIBLE HULLS USING MODULAR PROCEDURES

Irano Curvello Leite, iranocl@yahoo.com.br

Fernando Ribeiro da Silva, d4fernan@ime.eb.br

Instituto Militar de Engenharia, Praça General Tibúrcio, n. 80, Praia Vermelha, CEP 22290-270, Rio de Janeiro - RJ – Brazil

Abstract. *In the modeling of dynamic systems that include structural elements, the characterization of their interaction with other components may be very complex. Nevertheless, the use of power variables throughout the modeling procedure minimizes such problem, since the representation of the connections between the parts of a whole becomes simpler. The bond graphs modeling technique has been used for both lumped and distributed parameter systems, providing good results even for non-linear cases. Therefore, this work uses the generalization of the elements from such technique and the Finite Element Method to represent, through fields, the constitutive relations associated with structural members, facilitating their coupling with other components. The steps of the modeling procedure for a structural problem related to the dynamics of an armored vehicle with flexible hull, its natural frequencies and the corresponding mode shapes are shown. The simulation procedures use the representation of the bond graphs in the form of block diagrams, which also enhances the understanding of the models due to their modular feature, with the additional advantage of bypassing the development of state equations. The same vehicle was also modeled and simulated after assuming its hull as a rigid body and the time histories for some dynamic variables were, then, compared to the results obtained when considering structural flexibility.*

Keywords: *Bond Graphs, Block Diagrams, dynamic systems modeling, structural flexibility*

1. INTRODUCTION

The main purpose of this work is to study the influence of structural flexibility on the dynamic behavior of armored wheeled vehicles (personnel carriers, in particular) and the need to represent it when modeling hulls (armored vehicles bodies), comparing the differences between the results achieved by two distinct approaches to the same problem.

Some authors, like Zhang *et al.* (1998), state the importance and the necessity of including the component flexibility in conducting vehicle chassis/suspension dynamic analysis. In fact, the recent development of specific software packages for analysis and simulation of flexible multi-body dynamics, like ADAMS/FlexTM, seems to confirm that statement.

In addition, the following remarks can be done:

- Assuming that a vehicle structure is rigid is not always suitable, particularly for heavy military trucks, where flexibility becomes relevant due to the large deformations that their chassis may experience, especially under unusual dynamic conditions, like, for instance, during obstacle transpositions, driving through roads with rough uneven surfaces or off-road; and
- Modern armored vehicles require ever more intensive use of on board electronics, nearly always very sensitive to large accelerations and their time derivatives (jerks).

In this paper, the modeling and the simulation of two different situations involving the representation of the vertical dynamics of the same armored personnel carrier were conducted: in one case, a simplifying hypothesis was made such that the vehicle hull was thought of as being a rigid body; in the other case, those features related to the structural flexibility of the physical system proposed were introduced.

Thus, the vehicle structure was analyzed according to two different approaches:

- Rigid body dynamics (System 1); and
- Finite Element Method (System 2).

Both models were, then, simulated for a constant speed crossing of a speed bump type obstacle oblique to the displacement direction. In other words, both physical systems were subjected to the same base excitations and the time histories for some representative variables of each system were, then, compared.

The traditional approach usually requires a new memorial for each new project (even when it is based upon former developments) and for each modification to an existing project, since the change of a single parameter in a subsystem implies rewriting the entire set of equations used to describe the whole system dynamics.

To avoid that kind of difficulty, in this work the modeling tasks were conducted with the help of the procedures prescribed by the generalized bond graphs technique (Karnopp *et al.*, 1990), which proves to be quite attractive for the solution of a wide kind of engineering problems, on a wide field of the knowledge, even when dynamic subsystems of distinct natures interact to each other.

The bond graphs technique modularity permits of to model the different parts of a system independently and, after that, to join them together in a single graph by simply connecting them through suitable ports. Moreover, at any time, one can substitute or assemble subsystems in an existing model, without harming its functionality.

Particularly in this work, it's been used the generalization of the elements from such technique to represent, through fields, the constitutive relations associated with a deformable body, facilitating its coupling with other subsystems.

Notice that the concept of multibond graph for a generic structure, originally introduced by Da Silva and Speranza Neto (1993), was fully applied when modeling the hull in System 2. The methodology developed by those authors correlates the matrices of mass \mathbf{M} , stiffness \mathbf{K} and damping \mathbf{B} from the Finite Element Method, respectively, with inertia \mathbb{I} , compliance \mathbb{C} and resistive \mathbb{R} fields from the bond graphs technique.

As in Da Rocha (1998), the procedures of the bond graphs technique were used to perform the dynamic coupling of a structural subsystem (hull), represented using both lumped and distributed system assumptions, with eight lumped parameter subsystems (a driver plus his seat, an engine and six independent suspensions).

The simulations were made with Simulink™ (MathWorks Inc, 2007), commercial software package for signal processing that uses block diagrams architecture for physical systems representation.

Finally, to get the multiport fields models obtained through the bond graphs technique transformed into block diagrams, it's been used an approach developed by Ferreira and Da Silva (2005) and Ferreira (2006) that allows the modeling and simulation of almost every physical system without writing a single line of code to solve its state space equations.

2. MODELING

System 1 physical model, shown in Fig. 1a, comprises a driver plus his seat and an armored vehicle composed of an engine, one suspension for each of the six wheels and a rigid structure with three degrees of freedom, which correspond to pitch, bounce and roll motions.

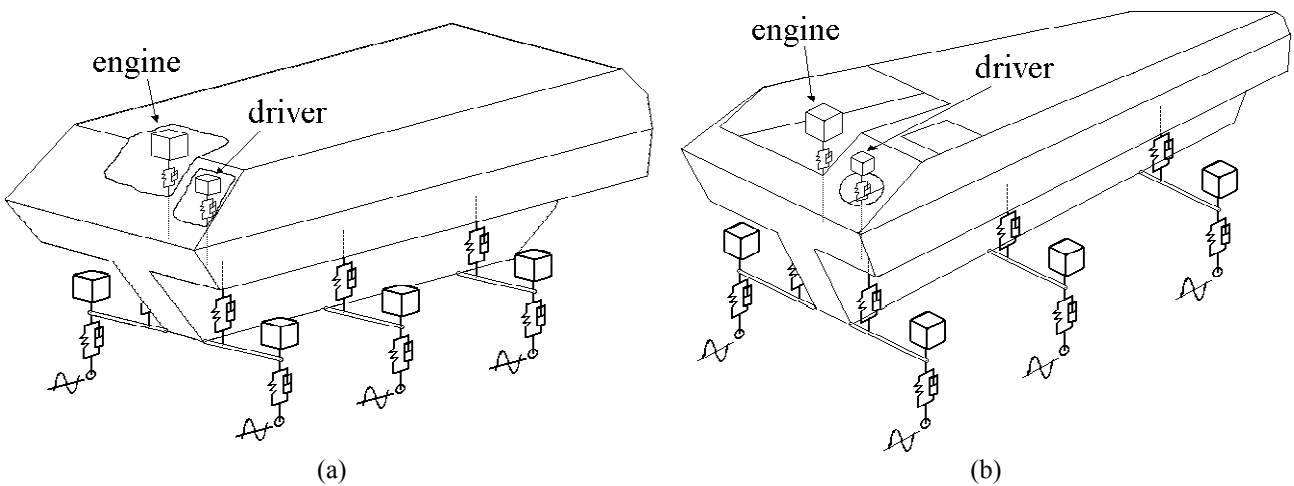


Figure 1. Physical models: (a) System 1; (b) System 2

System 2 physical model, shown in Fig. 1b, comprises a driver plus his seat and an armored vehicle composed of an engine, one suspension for each of the six wheels and a flexible structure discretized by means of 28 triangular and 212 rectangular shallow shell elements with six global degrees of freedom per node: one translation along and one rotation about each global coordinate axis. The elements, shown in Fig. 2, follow the classical Kirchhoff plate bending theory.

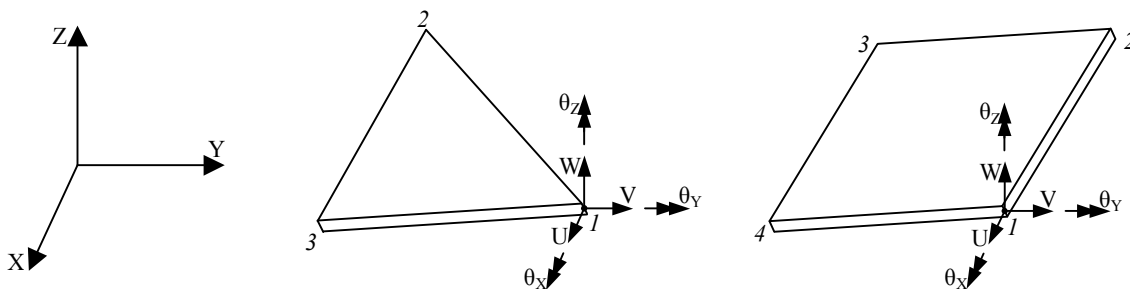


Figure 2. Shallow shell elements

Some of the constitutive parameters for the ballistic steel used to build the vehicle hull and the main physical properties of the hull itself are listed in Tab. 1 and 2, respectively.

Table 1. Ballistic steel constitutive parameters.

Elastic Modulus (GPa)	200
Poisson's ratio	0.3
Density (kg/m ³)	7860
Wall thickness (m)	0.0085

Table 2. Hull physical properties.

Mass (kg)	4041.72
Moment of inertia about x (kg·m ²) ⁽¹⁾	4173.49
Moment of inertia about y (kg·m ²) ⁽¹⁾	15175.96

⁽¹⁾: measured at a SAE vehicle axis system which originates at the center of mass of the hull

In both System 1 and System 2, the driver plus his seat and the engine have each been modeled as a rigid body supported by a spring and a damper possessing, respectively, mass, stiffness and damping properties as shown in Tab. 3 (throughout this work, only linear models for the constitutive relations have been used).

Table 3. Driver plus his seat and engine subsystems parameters.

Subsystem	Mass (kg)	Stiffness coefficient (N/m)	Damping coefficient (N·s/m)
Driver plus his seat	100	19620	1400
Engine	500	122625	24761

In both System 1 and System 2, the model for each of the six independent suspensions is composed of a shock absorber, a helical spring, a massless suspension arm and a wheel possessing mass, stiffness and damping properties as shown in Tab. 4.

Table 4. Suspension subsystems parameters.

Subsystem	Spring stiffness coefficient (N/m)	Shock absorber damping coefficient (N·s/m)	Wheel mass (kg)	Wheel stiffness coefficient (N/m)	Wheel damping coefficient (N·s/m)
Left front suspension	145300	25744	175	500000	140000
Right front suspension	145300	25744	175	500000	140000
Left middle suspension	345550	25744	175	500000	140000
Right middle suspension	345550	25744	175	500000	140000
Left rear suspension	602100	39656	175	500000	140000
Right rear suspension	602100	39656	175	500000	140000

Figures 3 and 4 show four mode shapes and natural frequencies for System 2. As normalization, it's been given the unitary value to the largest displacement of either the driver, the engine, or the hull nodes. The cubes drawn in solid lines represent the driver and the engine positions after deformation of the flexible elements. Furthermore, the suspension subsystems and the lateral walls of the hull haven't been represented, in order to get clearer sketches.

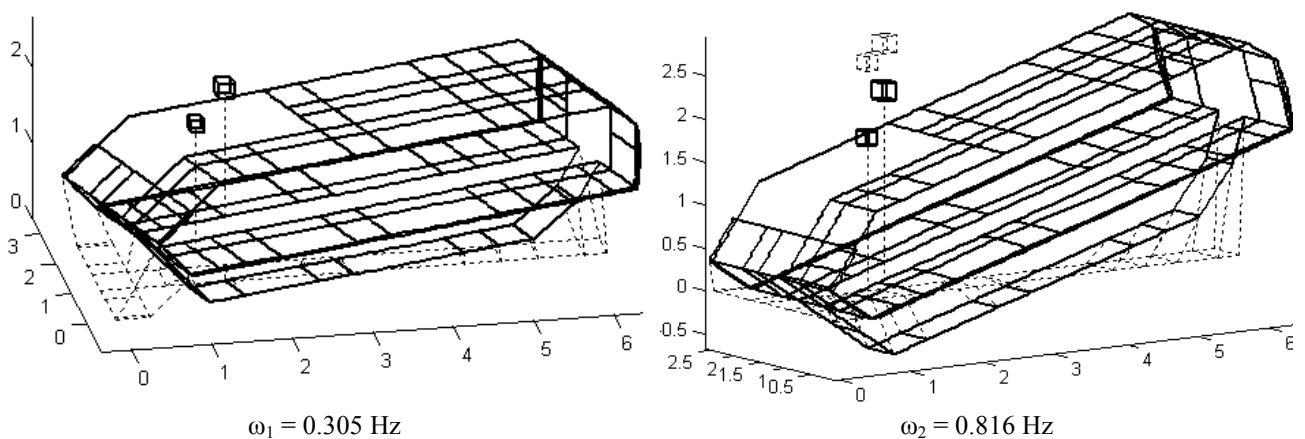


Figure 3. First two mode shapes and natural frequencies for System 2

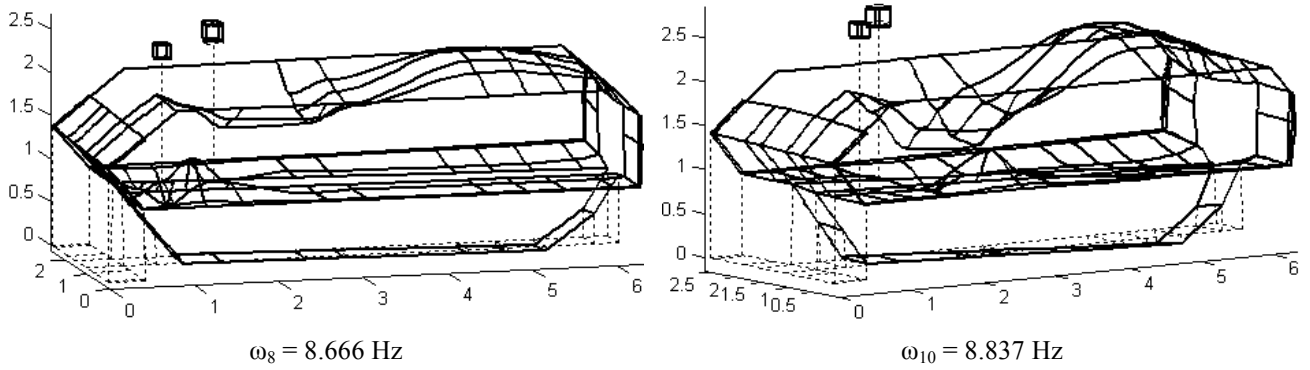


Figure 4. 8th and 10th mode shapes and natural frequencies for System 2

Figure 5 shows the bond graphs for both System 1 (dotted blue line) and System 2 (dashed red line), constructed by parts and assembled as in Da Rocha (1998). The upper-left and the upper-right parts of the figure represent the rigid and the flexible models of the hull, respectively. The lower-left part of the figure represents the driver plus his seat and the engine, while the lower-right side refers to the six suspension subsystems. The horizontal line denotes a composition (not a summation) of the vectors (flow and effort) contained in the three bonds from the non-structural subsystems (numbered from 19 to 21) into the vectors contained in the bonds numbered 6 (System 2) and 31 (System 1). Those numbers in square brackets indicate the dimensions of the vectors represented by each multibond.

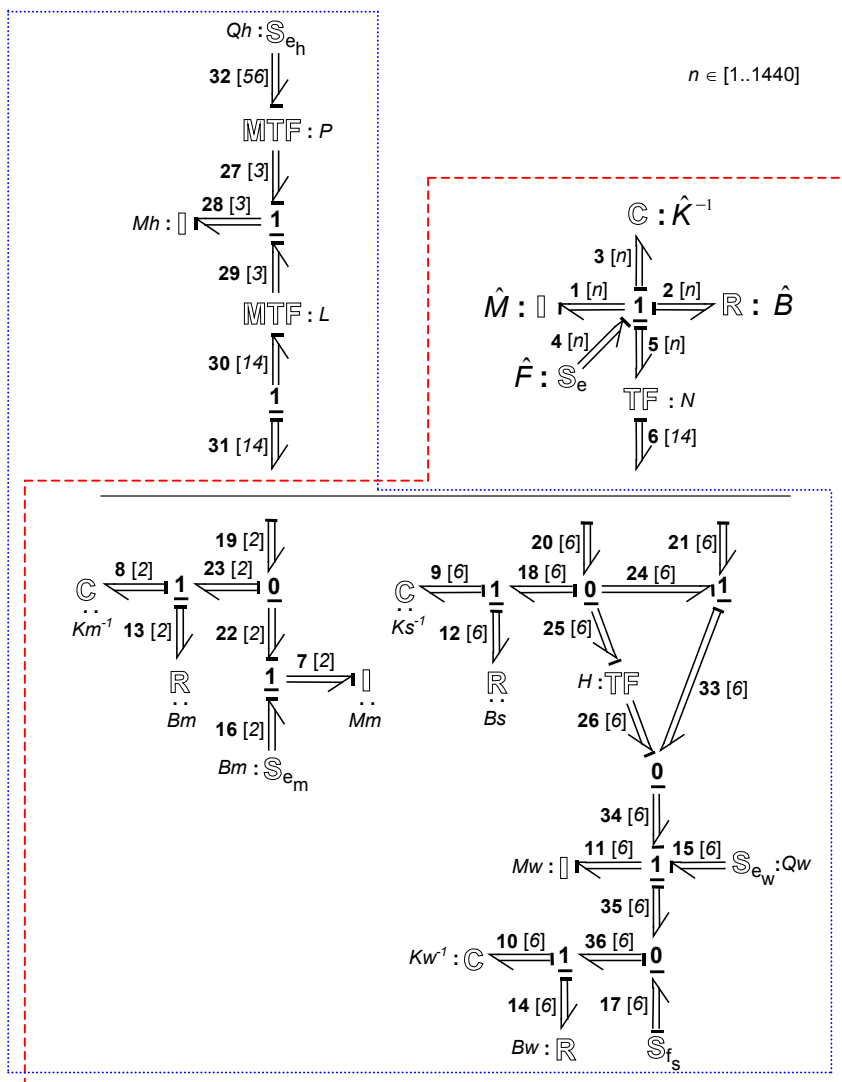


Figure 5. System 1 (blue dots) and System 2 (red dashes) multibond graphs

Figure 6 shows the block diagrams developed within Simulink™ from the bond graphs seen in Fig. 5, as in Ferreira and Da Silva (2005) and Ferreira (2006).

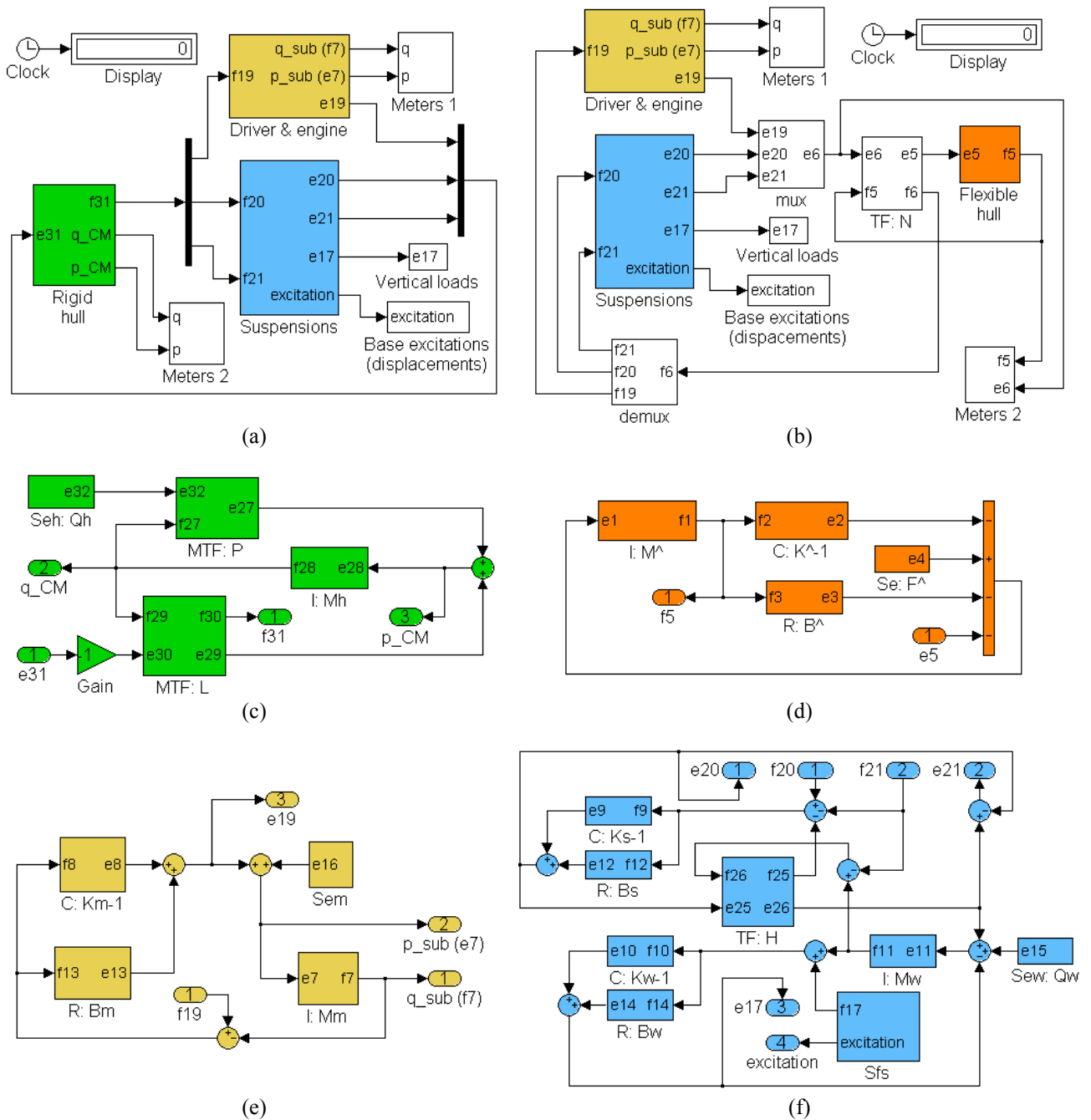


Figure 6. Block diagrams: (a) System 1; (b) System 2; (c) rigid hull; (d) flexible hull; (e) driver & engine; (f) suspensions

Figures 6(a) and (b) show the first hierarchic level of organization for Systems 1 and 2 block diagrams. Notice the use of the Simulink™ ability to group sets of related blocks into a major block when representing rigid hull, flexible hull, driver & engine and suspensions subsystems. The mux block is used to combine the signals corresponding to the efforts imparted to the hull by the non-structural subsystems, while the demux block splits the vector signal carrying the flows imparted to the driver plus his seat, the engine and the suspensions by the hull, exactly as the horizontal line in the bond graphs shown in Fig. 5. Finally, there are blocks with meters to which the signals one may want to analyze, treat or simply store are made to converge.

One level down the organizing hierarchy of the block diagrams referred to Systems 1 and 2 are those diagrams shown in Fig. 6c to 6f, which are nothing more than the content of the rigid hull (green), flexible hull (orange), driver & engine (yellow) and suspensions (blue) subsystems representative blocks, respectively.

3. SIMULATION

The simulation consisted of making the loaded vehicle models to travel on a road with a sine wave type obstacle (see Fig. 7a) laid out as shown in Fig. 7b. The simulated vehicle speed on the road surface, V_x , was 10 km/h.

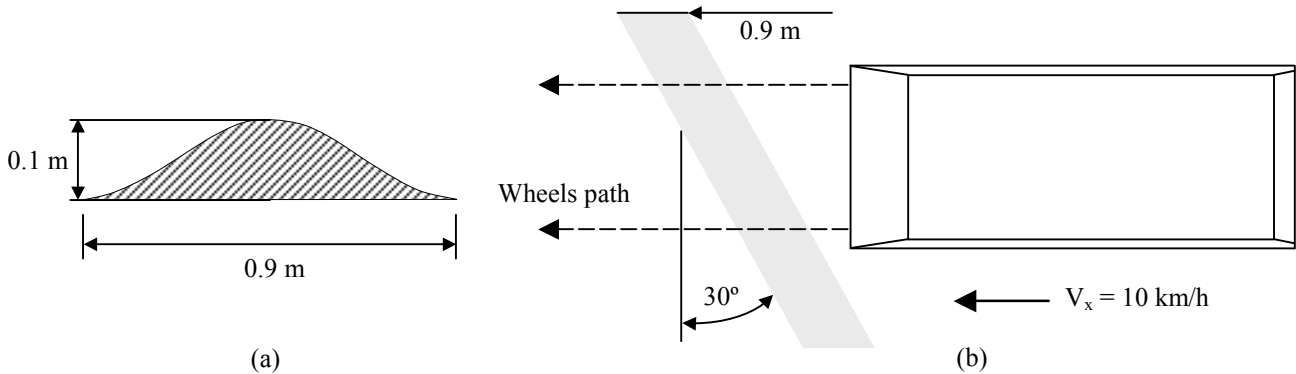


Figure 7. Obstacle: (a) normal cross section along vehicle wheels path; (b) top view layout

The weight of the load was added to the weight of the hull itself and the resulting value (117720 N) was equally divided by fifty six different points on the hull, each of them corresponding to those nodes in System 2 that are subjected to prescribed efforts.

Fifteen seconds of the vehicle dynamic behavior have been simulated. All the simulations started with null initial condition for every state variable. Since between three and four seconds were necessary for the system to achieve the steady state under the action of gravity, the vehicle starts to experience the base excitation only at the fifth second of simulation, when the left front wheel meets the obstacle. After the six wheels have crossed the obstacle, taking about three seconds, the rest of the simulation is spent for the vehicle to achieve the steady state again.

Since the ordinary differential equations system that defines the vehicle global mathematical model characterize a stiff problem, it's been used a most suitable solver among those in the assortment provided by Simulink™, ode15s, which proved to have the best performance in terms of CPU time.

3. RESULTS

Some of the results achieved with the simulation of the Simulink™ block diagrams developed for Systems 1 and 2 (see Fig. 6), are shown in this section.

Figure 8 shows the time histories for the normal reaction of the left front tire on the road, obtained from the 1st effort in multibond 17 of the graphs shown in Fig. 5, which corresponds to the 1st member of the vector signal e17 in the exit port 3 of the block diagram shown in Fig. 6f. Notice that such effort doesn't change its sign during simulation, otherwise meaning a tensile normal reaction, physically understood as the loss of contact of the tire to the ground.

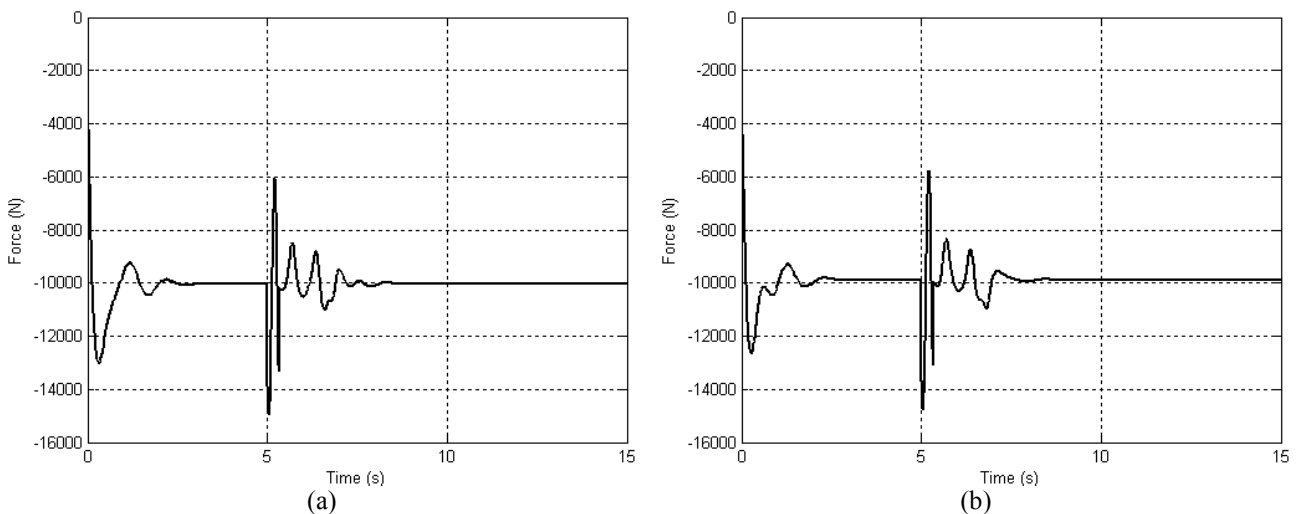


Figure 8. Normal reaction of the left front tire on the road: (a) System 1; (b) System 2

Figure 9 shows the time histories for the right front suspension spring vertical deformation, obtained from the time integration of the 2nd flow in multibond 9 of the graphs shown in Fig. 5, performed in SimulinkTM by taking to an integrator block the 2nd member of the vector signal f9, that enters block C: Ks-1 in the block diagram shown in Fig. 6f.

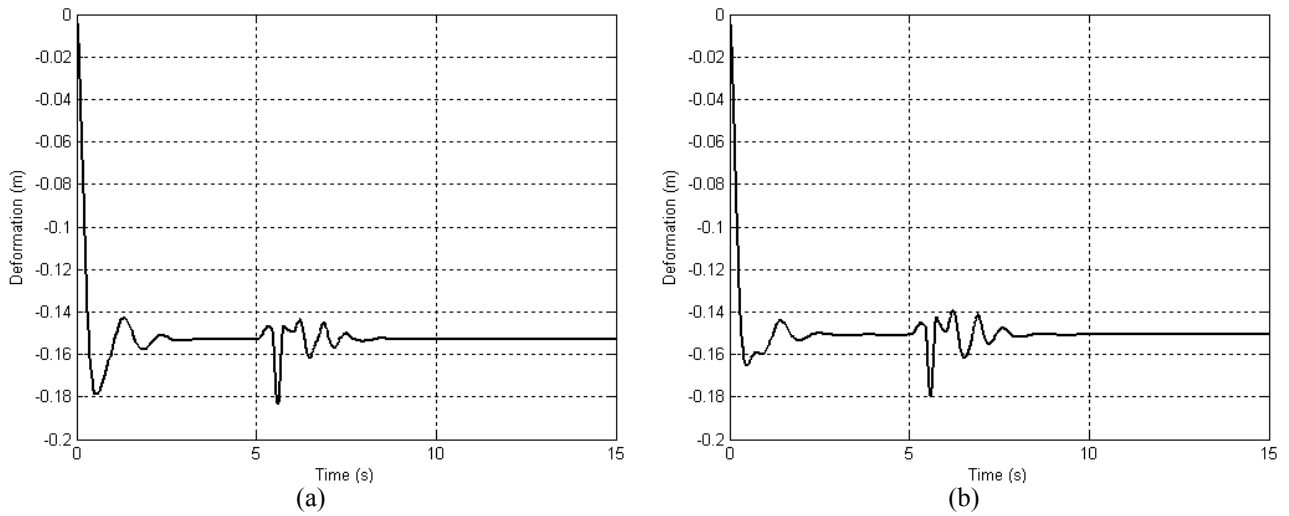


Figure 9. Right front suspension spring vertical deformation: (a) System 1; (b) System 2

The hull torsion angle is defined as the difference between the angles at which the lines at the front and rear edges of the hull slopes in relation to the horizontal plane. Since the System 1 hull is assumed, by hypothesis, to be rigid, its torsion angle will always be null, as shown in Fig. 10a.

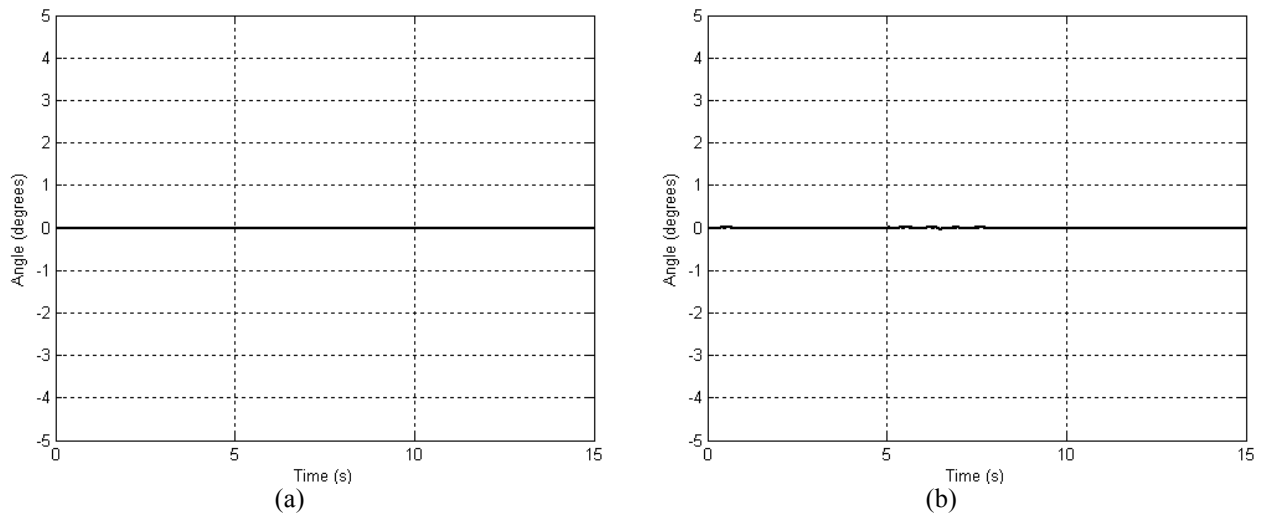


Figure 10. Hull torsion angle: (a) System 1; (b) System 2

Shown in Fig. 11 are the resulting time histories for the acceleration of the driver plus his seat from the simulations for the two different vehicle models, obtained from the 1st effort in multibond 7 of the graphs in Fig. 5 division by the mass of the driver plus his seat, performed in Simulink™ by taking to a gain block having gain parameter equal to the inverse of the mass of the driver plus his seat the 1st member of the vector signal e7, that enters block I: Mm in the block diagram shown in Fig. 6e.

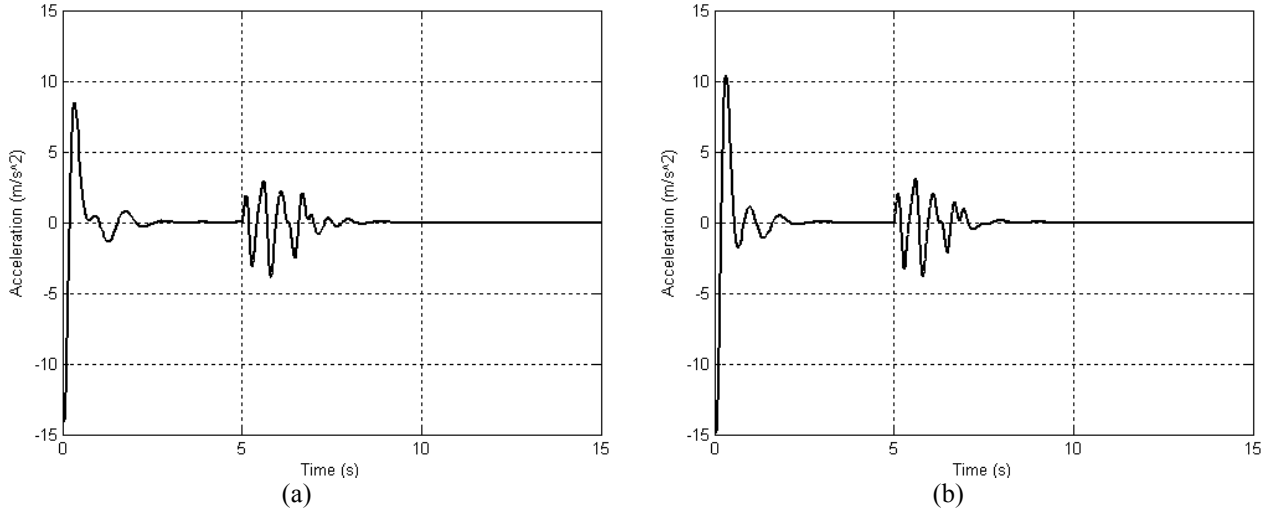


Figure 11. Acceleration of the driver plus his seat: (a) System 1; (b) System 2

Figure 12 shows, for the simulation period of time between 4 s and 10 s, the power dissipated by the left middle shock absorber, obtained from the 3rd result of the element-wise product of the effort vector times the flow vector in multibond 12 of the graphs shown in Fig. 5, which corresponds to the 3rd member of the vector signal leaving a product block whose entries are the vector signals e12 and f12, that connect to block R: Bs in the block diagram shown in Fig. 6f.

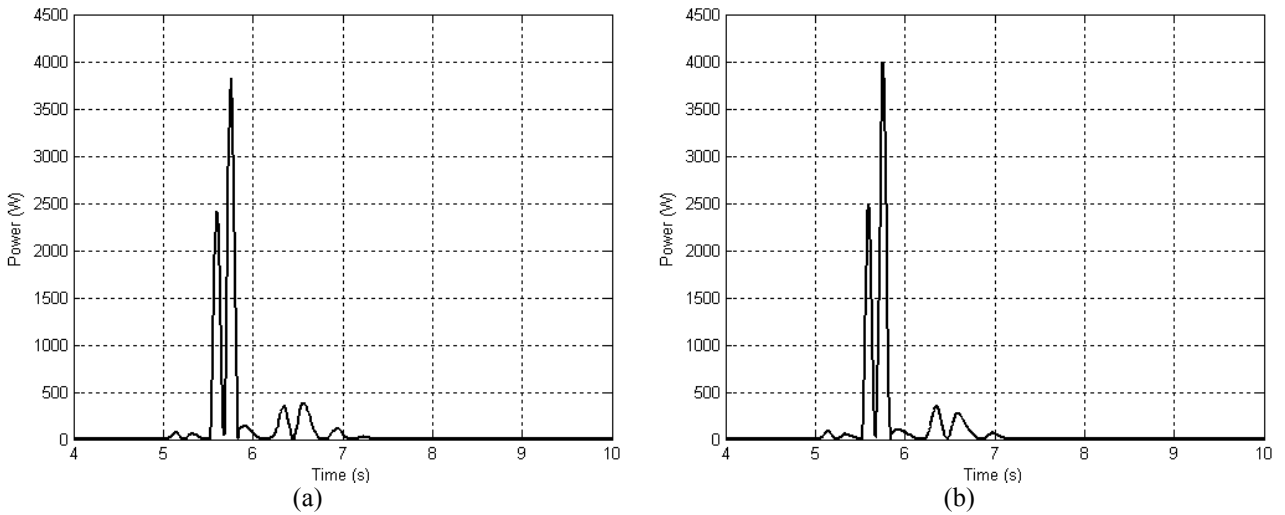


Figure 12. Power dissipated by the left middle shock absorber. (a) System 1; (b) System 2

Figure 13 shows the time histories for the right middle tire vertical deformation, obtained from the time integration of the 4th flow in multibond 10 of the graphs shown in Fig. 5, performed in SimulinkTM by taking to an integrator block the 4th member of the vector signal f10, that enters block C: Kw-1 in the block diagram shown in Fig. 6f.

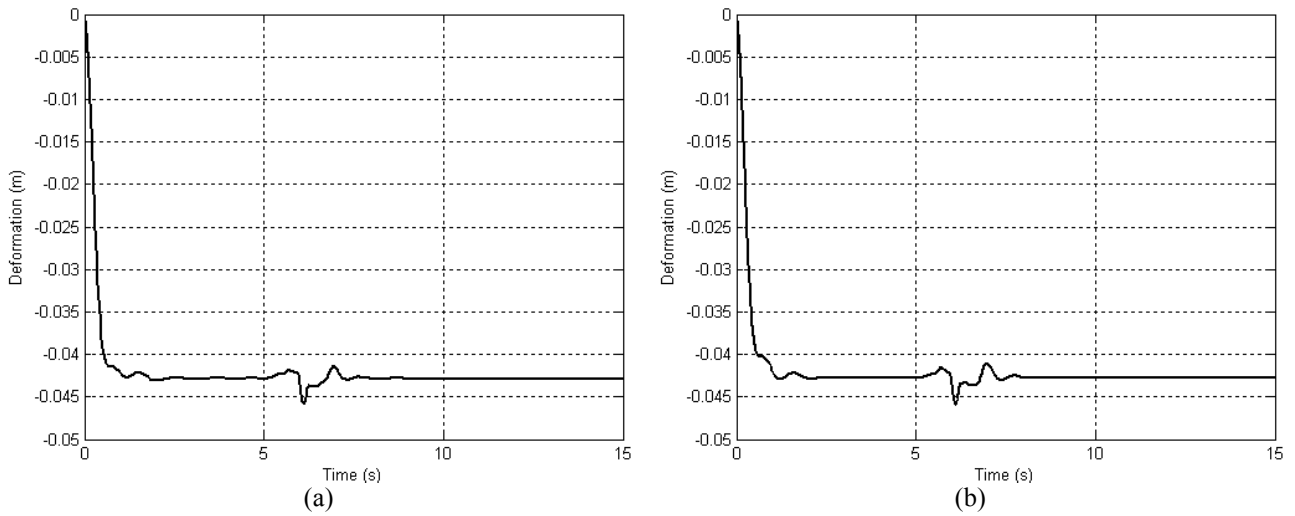


Figure 13. Right middle tire vertical deformation: (a) System 1; (b) System 2

Figure 14 shows, for the simulation period of time between 4 s and 10 s, the power dissipated by the left rear tire, obtained from the 5th result of the element-wise product of the effort vector times the flow vector in multibond 14 of the graphs shown in Fig. 5, which corresponds to the 5th member of the vector signal leaving a product block whose entries are the vector signals e14 and f14, that connect to block R: Bw in the block diagram shown in Fig. 6f.

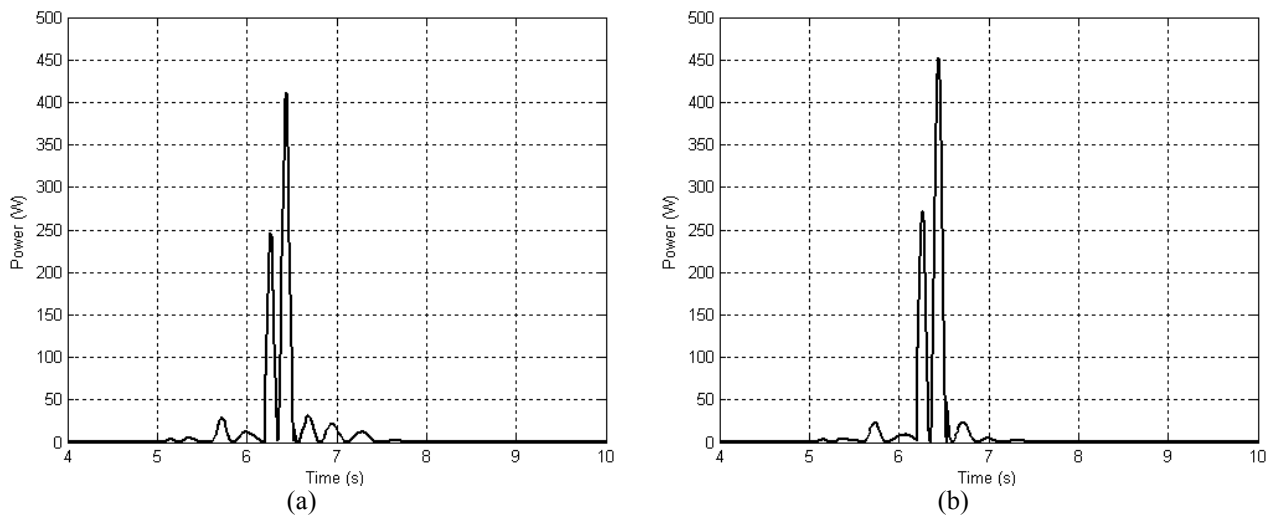


Figure 14. Power dissipated by the left rear tire: (a) System 1; (b) System 2

4. SUMMARY AND CONCLUSIONS

In the present paper, the effects of structural flexibility on an armored vehicle vertical dynamics were studied by means of a modular modeling procedure for deformable structures that uses the bond graphs technique generalized elements and a simulation environment with the concept of block diagrams.

In order to conduct the proposed analysis, it's been applied the flexible structures problem approach developed by Da Silva and Speranza Neto (1993), allowing dynamic models of structures discretized according to the Finite Element Method to be completely profited by the bond graphs technique, by using the generalization of the elements from such technique to represent, through fields, the constitutive relations of structural elements, whose coupling with the rest of their systems can, therefore, be more easily achieved.

The simulation procedures were conducted with the help of the models representation method developed by Ferreira and Da Silva (2005) and Ferreira (2006), allowing a dynamic system bond graph to be converted into a block diagram, which preserves all of the graph features and shows a schematic view of the studied system and of the relationship between its components, dispensing with the need to write any equation at all.

Finally, the rigid body dynamics and the finite element analyses of the vehicle hull have led to two different models. The dynamic simulation results for both cases mentioned above were then compared against each other to show the effects of structural flexibility upon the global vehicle dynamic behavior. However, no remarkable difference between the two sets of outputs was found (see Fig. 8 to 14). The most probable reason for that is the large stiffness inherent in all armored vehicles structures, caused by the large thickness of the sheets of steel used in their construction.

Therefore, at least for the simulations conducted in this work, it's been proved that the most important assumption in using the rigid body approach is valid: the global effect of the very small hull deformations, which are one or two order less than that of the springs, shocks, bushings, etc. (Zhang *et al.*, 1998) to the dynamic behavior of an armored vehicle is negligible.

Notice that it is not among the purposes of this paper the comparison with experiments or other works of the results presented herein, which are solely intended to give support to the analysis of the effects of structural flexibility upon armored wheeled vehicles dynamics. Anyway, one can see that, in general, the numeric results shown seem to be coherent, in terms of their order of magnitude.

Moreover, because of the modularity of both the modeling technique and the simulation tool, the models achieved can be easily sophisticated: not only the introduction of geometrical and/or physical non-linearities is feasible (for instance, with shock absorbers whose constitutive relations are taken from a force×speed type data bank) but also more complex structural models for the vehicle hull may be used without major difficulties.

5. REFERENCES

- Da Rocha, R.S., 1998, "Análise Dinâmica de Chassi Veicular Utilizando os Procedimentos Generalizados da Técnica dos Grafos de Ligação", Dissertação de Mestrado, IME, Rio de Janeiro, Brazil.
- Da Silva, F.R. and Speranza Neto, M., 1993, "Metodologia de Construção do Grafo de Ligação para Sistemas Estruturais", Proceedings of the 12th Brazilian Congress of Mechanical Engineering, Vol. 1, Brasília, Brazil, pp. 57-60.
- Ferreira, F.M. and Da Silva, F.R., 2005, "Computational Block-diagram Execution of Multiport Fields Models with Causal Considerations", Proceedings of the 18th Brazilian Congress of Mechanical Engineering, Ouro Preto, Brazil.
- Ferreira, F.M., 2006, "Modelagem de Sistemas Dinâmicos Utilizando Procedimentos Modulares", Dissertação de Mestrado, IME, Rio de Janeiro, Brazil.
- Karnopp, D.C., Margolis, D.L. and Rosenberg, R.C., 1990, "System Dynamics: A Unified Approach", John Wiley & Sons, New York.
- MathWorks Inc, 2007, "Matlab 7.0 User's Guide", Massachusetts, USA.
- Society of Automotive Engineers, 1952, "Vehicle Dynamics Terminology", SAE J670e, Warrendale, PA, USA
- Zhang, Y., Xiao, P., Palmer, T. and Farahani, A., 1998, "Vehicle Chassis/Suspension Analysis – Finite Element Model vs. Rigid Body Model", SAE Paper 980900, pp. 113-126.

6. RESPONSIBILITY NOTICE

The authors are the only responsible for the printed material included in this paper.